ISSN 1063-7842, Technical Physics, 2011, Vol. 56, No. 8, pp. 1147–1157. © Pleiades Publishing, Ltd., 2011.
Original Russian Text © Yu.I. Mankov, 2011, published in Zhurnal Tekhnicheskoĭ Fiziki, 2011, Vol. 81, No. 8, pp. 88–97.

RADIOPHYSICS

Electromagnetic Waves in a Randomly Inhomogeneous Josephson Junction

Yu. I. Mankov

Kirenskii Institute of Physics, Siberian Branch, Russian Academy of Sciences, Akademgorodok, Krasnoyarsk, 660036 Russia
e-mail: mankov@iph.krasn.ru

Received January 17, 2011

Abstract—Spectrum modification and damping of Josephson plasma waves induced by random inhomogeneities of the critical current through the superconductor contact and the averaged Green function of such excitations are analyzed. In the self-consistent approximation that makes it possible to take into account multiple wave scattering on the inhomogeneities, the frequency and damping of averaged waves, as well as position ν_m and peak width $\Delta\nu$ of the Fourier transform imaginary part of the averaged Green function, are determined as functions of wavevector k. The evolution of such functions with the variation of the correlation radius and the relative r.m.s. fluctuations of inhomogeneities is studied. The inhomogeneity-induced wave frequency decrease observed in the long wavelength spectral region qualitatively agrees with the ν_m behavior. It is established that in the case of "long-range" inhomogeneities, the linear dependence of damping on k changes to the inversely proportional one, and damping tends to zero as $k \longrightarrow 0$, while $\Delta\nu$ at small k attains its maximal values due to nonuniform broadening. In the presence of "short-range" inhomogeneities, the wave damping and $\Delta\nu$ are found to be similar functions of k. The results are compared to the numerical calculation data.

DOI: 10.1134/S1063784211080172

INTRODUCTION

Electromagnetic plasma-like excitations in Josephson junctions (Josephson plasma waves) have become a subject of extensive research. In some superconducting materials and structures, their frequency ranges from several hundreds of gigahertz to several tens of terahertz, i.e., falls into the intermediate range between the microwave and infrared spectral regions, and this makes promising the technical application of such excitations [1, 2]. Josephson plasma waves have been studied for a long time (see papers [3, 4] and reviews [1, 2]); however, in their analysis, the Josephson junction was assumed to be homogeneous. In real Josephson junctions, the superconductor contact is not perfect and has natural inhomogeneities which can, for example, be caused by spatial changes in the insulating layer thickness and in the composition of the dielectric layer, and inhomogeneity of the junction edges. Inhomogeneities can be artificially produced in the junctions. The inhomogeneity effect on electromagnetic excitations in the Josephson junction was studied for solitons (fluxons) which were considered in the presence of point [5–9] and periodic [10–14] inhomogeneities, as well as of regular nonperiodic [15] and random [16] inhomogeneities. Notwithstanding technological advances in the production of Josephson junctions, random inhomogeneities are always present there, and this makes it important to take into account these inhomogeneities when studying the electromagnetic excitations in these junctions. In particular, such studies are important for Josephson plasma waves because, as far as we know, the effect of random inhomogeneities on the plasma wave characteristics has not been studied despite ever increasing interest in these waves. In this work, we study the spectrum, damping, and the Green function of the Josephson plasma waves in a randomly inhomogeneous junction and determine their dependence on the stochastic parameters of the medium.

1. MODEL AND THE WAVE EQUATION

We consider two identical superconductors (Fig. 1) separated by a thin insulating layer of thickness w (superconducting tunnel junction). For the superconductor coherence length much larger than w, the Josephson electric current flows through the contact $j_z = j_c \sin\varphi$, where j_c is the Josephson junction critical current, and φ is the phase difference in the wave functions of superconducting electrons between the junction edges. It is known [3] that phase difference φ in a homogeneous Josephson junction in the absence of losses there is described by the equation

$$\frac{\partial^2\varphi}{\partial x^2} + \frac{\partial^2\varphi}{\partial y^2} - \frac{1}{c_0^2}\frac{\partial^2\varphi}{\partial t^2} = \frac{\sin\varphi}{\lambda_J^2}. \qquad (1)$$

Here, t is the time; $c_0 = c\sqrt{w/\varepsilon d}$ is the propagation velocity of electromagnetic waves in the junction (the Swihart velocity); c is the velocity of light in vacuum; ε is the junction dielectric permittivity; $d = w + 2\lambda$, where λ is the magnetic field penetration depth in the

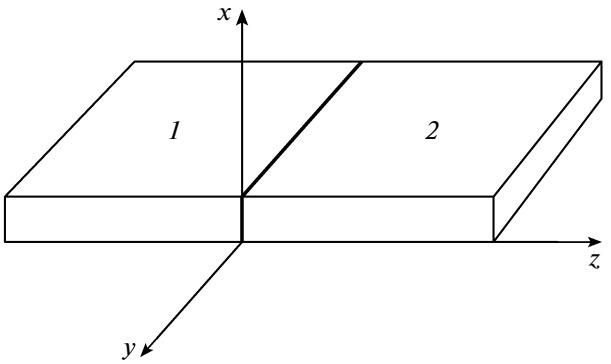

Fig. 1. System of coordinates. The origin of the z axis coincides with the position of the contact of superconductors *1* and *2*, parallel to the coordinate xy-plane.

superconductor; and λ_J is the Josephson penetration depth. In what follows, we will consider the "long" Josephson junction, $L_x \ll \lambda_J \ll L_y$ at $L_x \gg \lambda$, where L_x and L_y are the sample dimensions in the coordinate axes directions (see Fig. 1). In this model, phase difference φ depends weakly on variable x; therefore, the first term in Eq. (1) can be disregarded, and the equation turns to the one-dimensional sine-Gordon equation. In the general case, this equation has a soliton solution, and at small φ, it describes Josephson plasma waves.

In a randomly inhomogeneous Josephson junction, the physical quantities in Eq. (1) are random functions of the coordinates. To simplify the model, we assume, following [16], that velocity c_0 is uniform, and the Josephson penetration depth fluctuates,

$$\lambda_J^{-2}(y) = \lambda_J^{-2}[1 + \gamma\rho(y)], \qquad (2)$$

where $\rho(y)$ is the homogeneous random function with zero mathematical expectation ($\langle\rho\rangle = 0$) and the dispersion equal to unity ($\langle\rho^2\rangle = 1$); the angle brackets denote averaging over the realization ensemble of random function $\rho(y)$; and $\gamma = \Delta j_c/j_c$ is the r.m.s. fluctuation of the critical current, $0 \le \gamma < 1$.

Disregarding the first term on the left-hand side of Eq. (1), assuming $\varphi \ll 1$ therein, and performing the Fourier transformation with respect to time, we obtain

$$\frac{\partial^2\varphi(\omega, y)}{\partial y^2} + [\nu - \eta\rho(y)]\varphi(\omega, y) = 0, \qquad (3)$$

where $\nu = (\omega^2 - \omega_J^2)/c_0^2$, ω is the wave frequency, $\omega_J = c_0/\lambda_J$ is the Josephson plasma frequency, and $\eta = \gamma/\lambda_J^2$. In a homogeneous junction ($\gamma = 0$), Eq. (3) yields the following relation for the Josephson plasma wave spectrum:

$$\nu(k) = k^2, \qquad (4)$$

where k is the wavevector and $\varphi \propto \exp[i(ky - \omega t)]$. This dispersion law is shown by straight line $Q = 0$ in Figs. 2, 5, and 7. Expression (4) leads to the known formula for the wave spectrum,

$$\omega^2 = \omega_J^2 + c_0^2k^2. \qquad (5)$$

This relation is formally similar to the plasma wave spectrum; however, in the Josephson plasma wave, components E_z and H_x are other than zero like longitudinal component E_y of the electric field.

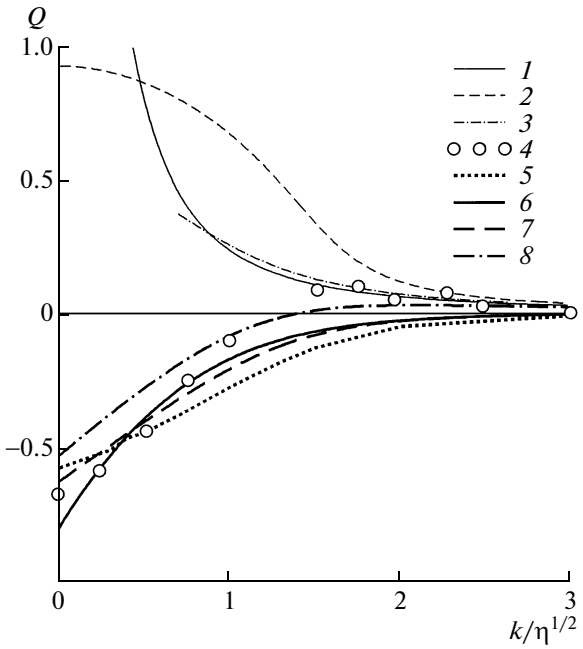

Fig. 2. Spectrum ν' of Josephson plasma waves and position of peak ν_m of function $|\bar{G}''(k, \nu)|$, $Q = (\nu' - k^2)/\eta$ (curve *1*), $Q = (\nu_m - k^2)/\eta$ (curves *2*–*8*); the formulas used to determine ν' and ν_m are given in the caption of Fig. 3; $k_c/\sqrt{\eta} = 0.5$.

2. GREEN FUNCTION, WAVE SPECTRUM, AND DAMPING

Analysis of Josephson plasma waves in a randomly inhomogeneous junction ($\gamma \ne 0$) requires that Eq. (3) should be considered approximately. We note that equations similar to Eq. (3), where the unknown and parameters are other physical quantities, describe the propagation of the waves of various types in various randomly inhomogeneous media. Therefore, we first of all touch upon the approximations and approaches that have been used earlier. If we use the perturbation theory proposed in [17] and similar to the Raleigh–Schrödinger theory, then simple analytical equations can be obtained for the wave spectrum and damping. Following this theory, we perform the Fourier transformation with respect to y in Eq. (3) and average it over the realization ensemble of random functions. As a result, after approximate uncoupling of correlation functions, we obtain the dis-

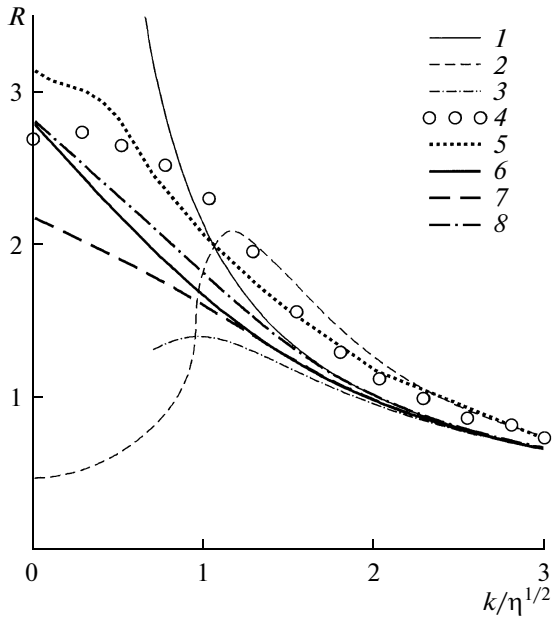

Fig. 3. Wave damping ν'' and width Δν of the peak of function $|\bar{G}''(k, \nu)|$, $R = 2\nu''/\eta$ (curve *1*), $R = \Delta\nu/\eta$ (curves *2*–*8*); (*1*) ν' and ν'' are defined by formula (8); (*2*, *3*) ν_m and Δν are respectively defined by formulas (12) and (13); (*4*) ν_m and Δν are obtained in [20]; ν_m and Δν are defined by (*5*) formulas (9), (16), and (18); (*6*) formulas (9) and (27); (*7*) formulas (9), (30), and (31); (*8*) formulas (9), (30), and (34); $k_c/\sqrt{\eta} = 0.5$.

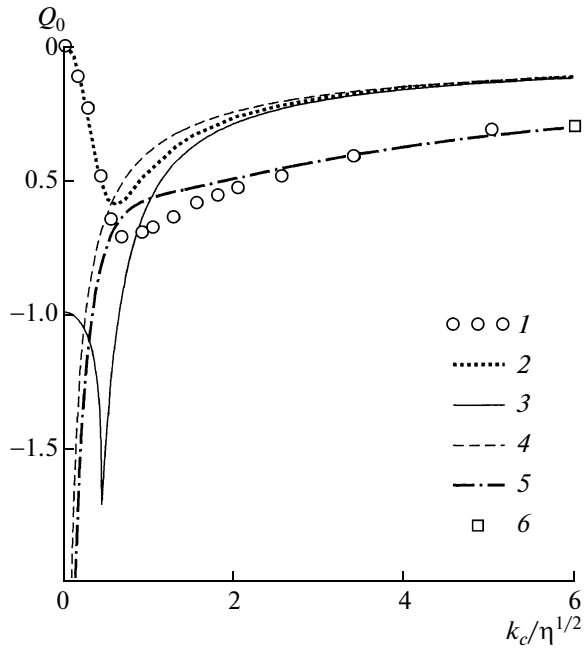

Fig. 4. Peak position ν_m of function $|\bar{G}''(k, \nu)|$ and frequency ν' of uniform oscillations, $Q_0 = \nu_m/\eta$ (curves *1*, *2*, *4*–*6*), $Q_0 = \nu'/\eta$ (curve *3*); $k = 0$; (*1*) ν_m was obtained in [20]; (*2*) ν_m is defined by formulas (9), (16), and (18); (*3*) ν' is defined by formula (20); (*4*) ν_m is defined by formulas (9), (30), and (31); (*5*) ν_m is defined by formula (35); (*6*) position of the point is determined by formulas (9) and (10).

persion relation for the averaged wave in the second order in γ ($\gamma^2 \ll 1$),

$$\nu(k) - k^2 = \eta^2 \int_{-\infty}^{\infty} \frac{S(k-k_1)}{k^2 - k_1^2} dk_1, \qquad (6)$$

where $S(k)$ is the spectral density Fourier-transform-related to correlation function $K_\rho(r) = \langle \rho(y)\rho(y+r)\rangle$ of inhomogeneities. The right-hand side of Eq. (6) determines the modification of the spectrum of the averaged wave and its damping. We consider the exponential damping of correlation functions

$$K_\rho(r) = \exp(-k_c|r|), \quad S(k) = \frac{k_c}{\pi(k_c^2 + k^2)}, \qquad (7)$$

where k_c is the correlation wavenumber of random inhomogeneities. The function ρ(*y*) and the correlation damping are assumed to be sufficiently smooth (correlation radius $r_c = 1/k_c \gg a$, where *a* is the interatomic distance). Applying formula (7) to expression (6) and integrating, we obtain

$$\nu(k) - k^2 = \eta^2 \frac{1}{k_c^2 + 4k^2} - i\eta^2 \frac{k_c^2 + 2k^2}{kk_c(k_c^2 + 4k^2)}. \qquad (8)$$

This relation was obtained in [17] for the elastic wave spectrum and damping in a fluctuating-density medium, $\nu(k) = \nu' - i\nu''$, where $\nu' = \mathrm{Re}\,\nu(k)$ and $\nu'' = -\mathrm{Im}\,\nu(k)$. Since $\nu(k)$ is an even function, here and in what follows only $k \geq 0$ are considered to simplify notation. The modification of the wave spectrum and its doubled damping following from expression (8) are shown in Figs. 2 and 3 (curves *1*). At $k \ll k_c$, the wave damping $\nu'' \propto 1/k$, and this imposes some constraints on the application of formula (8).

The averaged waves in a randomly inhomogeneous medium can be described in more detail in the Kraichnan approximation [18], which is usually called the self-consistent approximation [19] and takes into account multiple wave scattering on inhomogeneities. According to the approach described in [18, 19], Fourier transform $\bar{G}(k, \nu)$ of the averaged Green function corresponding to Eq. (3) has the form

$$\bar{G}(k, \nu) = \frac{(2\pi)^{-1}}{\nu - k^2 - \Sigma(k, \nu)}, \qquad (9)$$

where mass operator $\Sigma(k, \nu)$ is defined by the integral equation

$$\Sigma(k, \nu) = \eta^2 \int_{-\infty}^{\infty} \frac{S(k-k_1)dk_1}{\nu - k_1^2 - \Sigma(k_1, \nu)}. \qquad (10)$$

The authors of [20] also proposed a simple derivation of this formula. The Green function is proportional to

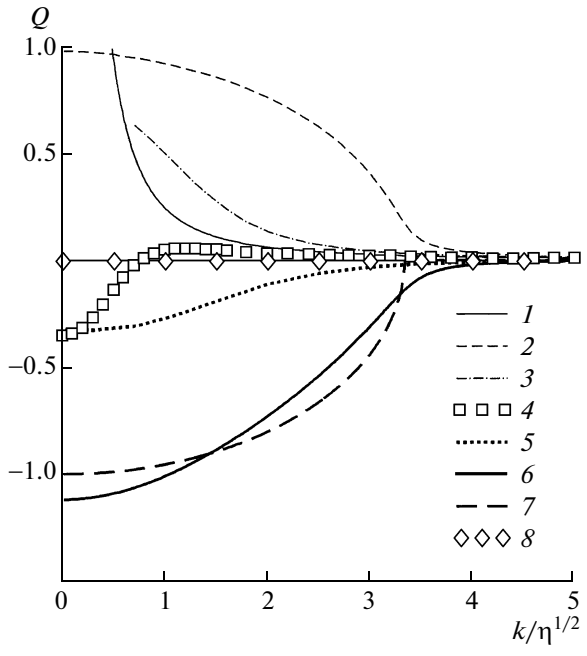

Fig. 5. Spectrum ν' of Josephson plasma waves and position of peak ν_m of function $|G''(k, \nu)|$, $Q = (\nu' - k^2)/\eta$ (curves *1–3*, *6*, *7*), $Q = (\nu_m - k^2)/\eta$ (curves *4*, *5*, *8*), the formulas used to define ν' and ν_m are given in the caption to Fig. 6; $k_c/\sqrt{\eta} = 0.3$.

the high-frequency susceptibility, and zero denominator of function $\bar{G}(k, \nu)$ gives dispersion relation for the averaged wave,

$$\nu(k) = k^2 + \Sigma(k, \nu(k)). \quad (11)$$

Self-consistent equation (10) can be solved numerically. To obtain $\Sigma(k, \nu)$ in analytic form (in particular, for determining the wave spectrum and damping), the simplifications are used, which allow one to evaluate the integral on the right-hand side of Eq. (10).

If we assume that $\Sigma(k_1, \nu) = 0$ in the integrand of Eq. (10), which is justified for $\gamma^2 \ll 1$, then the formula for the mass operator can be obtained in the Bourret approximation [21], and the Fourier transform of the averaged Green function has the form

$$\bar{G}(k, \nu) = \frac{(2\pi)^{-1}}{\nu - k^2 - \dfrac{\eta^2}{(\sqrt{\nu} + ik_c)^2 - k^2}\left(1 + \dfrac{ik_c}{\sqrt{\nu}}\right)}. \quad (12)$$

The Bourret approximation is widely used in analysis of equations similar to Eq. (3). This approach was applied for determining the characteristics of electromagnetic waves in a randomly inhomogeneous medium [22] and of spin waves in amorphous ferromagnets with a fluctuating anisotropy parameter [20]. If we use the equality $\nu = k^2$ along with the condition $\Sigma(k_1, \nu) = 0$ in the integrand of Eq. (10), then the mass operator will be determined by the right-hand side of formula (6). In the latter case, the mass operator depends only on wavevector k; i.e., in accordance with relation (11), $\Sigma'(k)$ determines the wave spectrum modification, while $\Sigma''(k)$ determines its damping: $\nu' - k^2 = \Sigma'(k)$, $\nu'' = -\Sigma''(k)$, where $\Sigma'(k) = \mathrm{Re}\Sigma(k)$, $\Sigma''(k) = \mathrm{Im}\Sigma(k)$. We also recall that, at $\Sigma(k, \nu) \equiv \Sigma(k)$, expression (9) yields $\nu_m = \nu'$ and $\Delta\nu = 2\nu''$, where ν_m is the frequency for which function $|\bar{G}''(k, \nu)|$ attains its maximum value at the given value of k or the position of the peak of function $|\bar{G}''(k, \nu)|$, and $\Delta\nu$ is the half-height width of this peak; $\bar{G}''(k, \nu) = \mathrm{Im}\bar{G}(k, \nu)$. If the mass operator is a function of both ν and k, then, on the whole, there is only qualitative correspondence between ν_m and ν' as well as $\Delta\nu$ and $2\nu''$. This situation arises, in particular, in the Bourret approximation.

One more simplification method for Eq. (10) was proposed in [20]. In this method, $\Sigma(k, \nu)$ is substituted for $\Sigma(k_1, \nu)$ in the integrand of Eq. (10). In this approximation, under the additional condition $|\Sigma(k, \nu)| \ll \nu, k$, expressions (9) and (10) yield the following relation:

$$\bar{G}(k, \nu) = \frac{(2\pi)^{-1}}{\nu - k^2 - P + i\left(\eta^2 \dfrac{\sqrt{\nu} + ik_c}{\sqrt{\nu}} - P^2\right)^{1/2}}, \quad (13)$$

where $P = [(\sqrt{\nu} + ik_c)^2 - k^2]/2$. The positions ν_m of the peak of function $|\bar{G}''(k, \nu)|$, where $\bar{G}(k, \nu)$ is defined by relations (12) and (13), are presented in Fig. 2 (curves *2*, *3*), while peak width $\Delta\nu$ is presented in Fig. 3 (curves *2*, *3*). Figure 2 demonstrates that the use of approximate expressions (8), (12), and (13) to describe averaged waves in a randomly inhomogeneous medium gives the displacement of the peak of $|\bar{G}''(k, \nu)|$ to higher frequencies relative to its position when the waves propagate in a homogeneous medium. Meanwhile, the numerical calculations [20] performed in the self-consistent approximation give (at low values of the wavevector k, for which the spectrum modification is the strongest) the displacement of ν_m to lower frequencies (the sequence of points *4* in Fig. 2). At relatively high k, curves *1–3* in Fig. 2 adequately approximate the behavior of the sequence of points *4*. The latter circumstance relates equally to curves *1–4* in Fig. 3. However, at low k, the peak width $\Delta\nu$ calculated in [20] (the sequence of points *4* in Fig. 3) also differs considerably from its values following from relations (8), (12), and (13) (curves *1–3* in Fig. 3). Therefore, comparison of the averaged Green function obtained by numerical calculation of integral equation (10) and approximate formulas (8), (12), and (13) leads to the conclusion that these formulas do not suffice to correctly describe the spectrum modification of averaged waves and their damping. Hence, an approach should be found which allows one to obtain

the expression for the Green function, which agrees with the results of numerical calculation and makes it possible to find the dispersion relation for averaged waves in a randomly inhomogeneous medium.

We note that, according to relation (7), function $S(k - k_1)$ in the integrand of Eq. (10) reaches its maximum at $k_1 = k$. This means that the neighborhood of point $k_1 = k$ makes the major contribution to the integral of Eq. (10). Therefore, we present the denominator of the integrand of Eq. (10) as a power series

$$\nu - k_1^2 - \Sigma(k_1, \nu) = g - \left[2k + \frac{d\Sigma(k, \nu)}{dk}\right](k_1 - k) - \left[1 + \frac{1}{2}\frac{d^2\Sigma(k, \nu)}{dk^2}\right](k_1 - k)^2 - \ldots, \quad (14)$$

where $g = \nu - k^2 - \Sigma(k, \nu)$. Substituting expansion (14) into relation (10) and retaining only the first two terms therein, we integrate the result, using formula (7) for the spectral density at $k_c \neq 0$. This gives

$$\Sigma(k, \nu) = \frac{\eta^2}{g + ik_c\left[2k + \frac{d\Sigma(k, \nu)}{dk}\right]}. \quad (15)$$

Unfortunately, we have failed to solve the differential equation that follows from the above expression; for this reason, we consider it as an algebraic equation in $\Sigma(k, \nu)$. In this case, the formal solution to Eq. (15) is

$$\tilde{\Sigma}(k, \nu) = \frac{1}{2}(X + iK_cY) - i\sqrt{1 - \frac{1}{4}(X + iK_cY)^2}, \quad (16)$$

where we have introduced the following dimensionless quantities:

$$Y = \frac{2k + \frac{d\Sigma(k, \nu)}{dk}}{\sqrt{\eta}}, \quad K = \frac{k}{\sqrt{\eta}}, \quad K_c = \frac{k_c}{\sqrt{\eta}}, \quad \tilde{\Sigma}(k, \nu) = \frac{\Sigma(k, \nu)}{\eta}, \quad X = \frac{\nu - k^2}{\eta}. \quad (17)$$

Expression (15) was obtained for $\mathrm{Im}(\tilde{g}/Y) > 0$, where $\tilde{g} = g/\eta$. To find unknown Y in relation (16), it is differentiated with respect to k. Then, considering the definition of Y and assuming that $|d^2\Sigma(k, \nu)/dk^2| \ll 1$, we obtain

$$Y = K + iK_c - \frac{i}{2}\frac{(X + iK_cY)(K - iK_c)}{\sqrt{1 - \frac{1}{4}(X + iK_cY)^2}}. \quad (18)$$

Substituting the numerical solution to this equation for Y into expression (16), we obtain the mass operator values which, being substituted into relation (9), allow us to determine the position ν_m and width $\Delta\nu$ of the peak of function $|\bar{G}''(k, \nu)|$ shown, respectively, by curves *5* in Figs. 2 and 3. These figures illustrate the closeness of both the $\nu_m(k)$ and $\Delta\nu(k)$ dependences determined using expressions (9), (16), and (18) and calculated in paper [20] (cf. the sequences of points *4* and curves *5* in Figs. 2 and 3). Formulas (16) and (18) yield $|d^2\Sigma(k, \nu)/dk^2|/2 < 0.3$. Let us now consider an important case of uniform oscillations ($k = 0$). Figure 4 presents the dependence of ν_m on correlation wavenumber k_c obtained in [20] (the sequence of points *1*), as well as the dependence of ν_m on k_c following from expressions (9), (16), and (18) (curve *2*). We notice the coincidence of curves *1* and *2* in Fig. 4 at $K_c \leq 0.4$ and the qualitative agreement of their behavior in the remaining range of values of k_c. The closeness of the numerical results for the Green function obtained in the approach being developed in this paper and in [20] substantiates the application of expressions (16) and (18) to determine the spectrum and damping of the averaged wave; it also indicates that using expansion (14) in expression (10), we still remain within the self-consistent approximation limits.

Let us now calculate the wave spectrum and damping. Formula (11) subject to notation (17) has the form $\tilde{\Sigma}(k, \nu) = X$. Using this equality in relation (16), we get a system of two nonlinear equations in two unknowns, X and Y, which leads to the cubic equation for X,

$$X^3 + \frac{1}{2K_c^2}X^2 + \frac{iK}{K_c}X - \frac{1}{2K_c^2} = 0. \quad (19)$$

Only one of its solutions has physical sense,

$$X = \frac{1}{12K_c^2}\left[\frac{(1 - i\sqrt{3})(12iKK_c^3 - 1)}{D_1^{1/3}} - (1 + i\sqrt{3})D_1^{1/3} - 2\right], \quad (20)$$

where

$$D_1 = 18K_c^3(3K_c + iK) - 1 + 6\sqrt{3}K_c^3 \times \sqrt{K_c^2(K^2 + 18iKK_c + 27K_c^2) - 16iK^3K_c^5 - 1}. \quad (21)$$

The spectrum of averaged wave ν' and its doubled damping $2\nu''$, which follow from relation (20), are shown for $K_c = 0.3$ by curves *6* in Figs. 5 and 6, respectively, and for $K_c = 0.5$, by curves *6* in Figs. 7 and 8, respectively. Therefore, we obtained a decrease in the frequency of the averaged waves in a randomly inhomogeneous medium as compared to its values in a homogeneous junction. This correlates with the displacement to lower frequencies of position ν_m of the peak of function $|\bar{G}''(k, \nu)|$ numerically calculated from expressions (9) and (10) (the sequences of points *4* in Figs. 5 and 7) and based on formulas (9), (16), and (18) (curves *5* in Figs. 5 and 7). At the same time, the spectrum modification that follows from approximate formulas (8), (12), and (13) obtained in the perturbation theory and is represented by curves *1*, *2*, and *3* in Figs. 5 and 7, respectively, lies in an increase in the averaged wave frequency. We note that under considerable modification of the spectrum in the long-wavelength region where $(\nu' - k^2)/\eta < -1$, the spectral

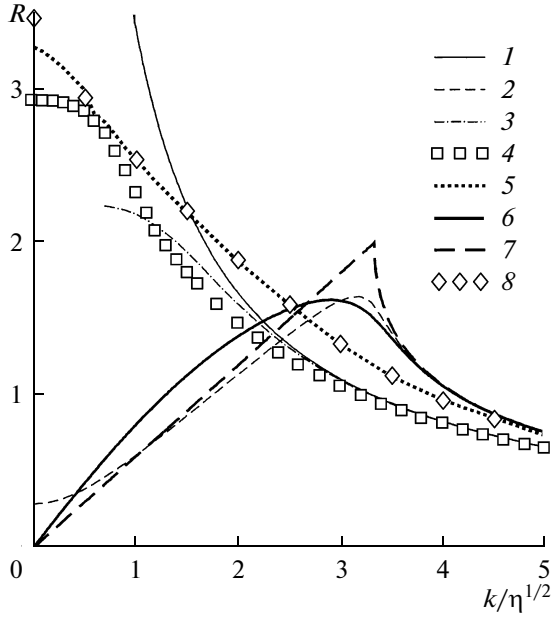

Fig. 6. Wave damping ν'' and width Δν of the peak of function $|\bar{G}''(k, \nu)|$, $R = 2\nu''/\eta$ (curves *1–3*, *6*, *7*), $R = \Delta\nu/\eta$ (curves *4*, *5*, *8*); (*1–3*) ν' and ν'' are defined by formulas (8), (12), and (13); (*4*) ν_m and Δν are defined by formulas (9) and (10); (*5*) ν_m and Δν are defined by formulas (9), (16), and (18); (*6*, *7*) ν' and ν'' are respectively defined by formulas (20) and (37); (8) ν_m and Δν are defined by formulas (9) and (15) and the derivative with respect to k of Eq. (10); $k_c/\sqrt{\eta} = 0.3$.

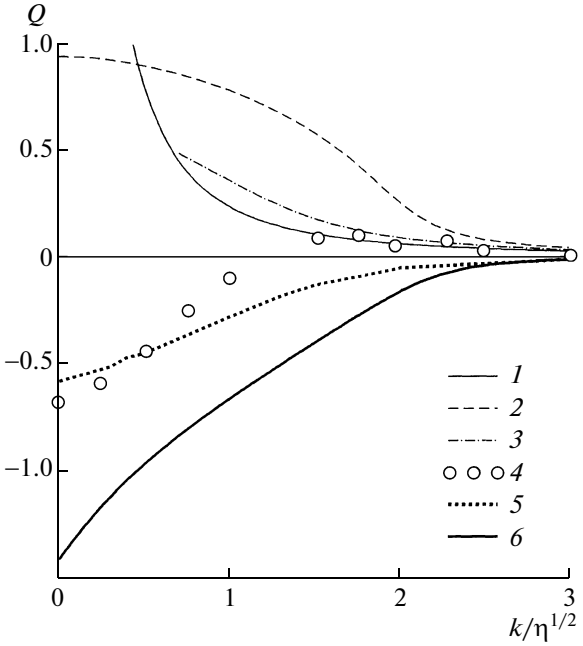

Fig. 7. Spectrum ν' of Josephson plasma waves and position of peak ν_m of function $|G''(k, \nu)|$, $Q = (\nu' - k^2)/\eta$ (curves *1–3*, *6*, *7*), $Q = (\nu_m - k^2)/\eta$ (curves *4*, *5*), the formulas used to define ν' and ν_m are given in the caption to Fig. 8, $k_c/\sqrt{\eta} = 0.5$.

curve is within the peak width Δν of function $|\bar{G}''(k, \nu)|$. The $\Delta\nu(k)$ dependence numerically calculated from expressions (9) and (10) is respectively presented in Figs. 6 and 8 at $K_c = 0.3$ and $K_c = 0.5$ by the sequences of points *4*, while curves *5* in these figures illustrate the behavior of Δν following from formulas (9), (16), and (18). Comparing the shapes of curves *6* in Figs. 6 and 8 implies that the averaged wave damping is considerably transformed at a small change in K_c. In mathematical terms, it is conditioned by that the radicand in formula (21) changes its sign upon an increase in K_c. For example, for uniform oscillations ($K = 0$), the sign reversal occurs at $K_c = K_{c0} \equiv 27^{-1/4} \approx 0.4387$, i.e., at $k_c = k_{c0}$, where $k_{c0} = K_{c0}\sqrt{\gamma}/\lambda_J$ is the critical value of the correlation wavenumber. As a result, if $K_c < K_{c0}$, the damping tends to zero as $K \longrightarrow 0$, while if $K_c > K_{c0}$, the damping remains finite for $K \longrightarrow 0$. The former inequality yields the condition $r_c \gg \lambda_J$ under which the inhomogeneities have a weak effect on the wave propagation; however, if r_c is lower than or on the order of λ_J, this effect becomes stronger, and the damping of averaged waves increases. According to Figs. 6 and 8, peak width Δν and doubled wave damping 2ν'' depend differently on k (cf. curves *5* and *6* in these figures). This is due to the fact that Δν (calculated in the self-consistent approximation, as noted in [20]) is determined, apart from the wave damping, by a nonuniform (fluctuation) broadening associated with a stochastic spread in the values of the randomly inhomogeneous parameter. Therefore, curves *4* and *5* in Figs. 6 and 8 illustrate the joint effect of these two mechanisms. The averaged wave damping obtained in this paper from Eq. (20) makes it possible to estimate the contribution of each mechanism. Comparing Δν (the sequence of points *4* and curve *5* in Figs. 6 and 8) with 2ν'' (curves *6* in Figs. 6 and 8), we conclude that at small k_c, the nonuniform broadening contribution to peak width Δν of function $|\bar{G}''(k, \nu)|$ prevails in the range $K \ll 1$, while the contribution of the wave damping becomes predominant for $K \gg 1$. A slight increase in 2ν'' above Δν is apparently due to the approximations used in the derivation of Eq. (18). We notice that the dependences of Δν and 2ν'' on k obtained in the Bourret approximation are also different (see curves *2* in Figs. 3 and 8).

In the limiting cases, expression (20) that describes the spectrum and damping of averaged Josephson plasma waves is simplified. We note that for $\gamma \longrightarrow 0$, Eq. (20) yields the equality $X = 0$, and then, formulas (4) and (5) for the wave spectrum in a homogeneous medium. If $\gamma \neq 0$ and $K \ll 1$, $K_c \ll 1$, using definitions (17) in expression (20), we obtain

$$\omega^2 \approx \omega_J^2(1 - \gamma - k_c^2\lambda_J^2) + c_0^2k^2 - ic_0^2kk_c. \qquad (22)$$

Here, $\omega = \omega' - i\omega''$, where ω' and ω'' describe, respectively, the averaged wave spectrum and damping. Since the inequality $K_c \ll 1$ is equivalent to the condition $k_c^2\lambda_J^2 \ll \gamma$, it follows from formula (22) that a decrease in the gap of the wave spectrum depends on parameter γ. Meanwhile, the wave damping is a linear function of k and k_c. At $K \ll 1$ and $K_c \gg 1$, we have from expression (20)

$$X \approx -\frac{1+i\sqrt{3}}{(4K_c)^{2/3}} + \frac{\sqrt{3}+i}{3(4K_c)^{1/3}}K + \frac{2^{1/3}(1-i\sqrt{3})}{54K_c^{4/3}}K^2, \quad (23)$$

and turning back to the dimensional quantities, we obtain the following expression for the wave spectrum and damping:

$$\omega^2 \approx \omega_J^2\left[1 - \gamma^{4/3}\frac{1+i\sqrt{3}}{(4\lambda_J k_c)^{2/3}} + \gamma^{2/3}\frac{\sqrt{3}+i}{3(4\lambda_J k_c)^{1/3}}\lambda_J k\right] + \left[1 + \gamma^{2/3}\frac{2^{1/3}(1-i\sqrt{3})}{54(\lambda_J k_c)^{4/3}}\right]c_0^2k^2. \quad (24)$$

Formula (24) implies that in a randomly inhomogeneous junction at high k_c values, the wave damping is proportional to $\propto 1/k_c^{2/3}$. This dependence was singled out numerically in [20] for the ferromagnetic resonance line width and had been predicted earlier by scaling (see references in [20]). Finally, at $k \gg k_c$, we find from expression (20) subject to definitions (17) that

$$\omega^2 \approx \omega_J^2\left(1 - \frac{\gamma^4}{k^4k_c^2\lambda_J^6} - i\frac{\gamma^2}{2kk_c\lambda_J^2}\right) + c_0^2k^2. \quad (25)$$

The wave damping following from expression (25) coincides with that following (at large k) from formula (8) obtained in perturbation theory. Relations (22), (24), and (25) show that the use of the first two terms of expansion (14) in Eq. (10) yields, at arbitrary wavevector values, a decrease in averaged wave frequency as compared to the frequency value in a homogeneous junction. We investigate in more detail the dependence of the wave spectrum on the correlation wavenumber for homogeneous ($k = 0$) oscillations. Curve *3* in Fig. 4 presents the averaged wave frequency ν' as a function of k_c which we obtain from relation (20) at $K = 0$. A sharp minimum on this curve is at $K_c = K_{c0}$. Figure 4 demonstrates that at large K_c, curves *2* and *3* coincide; i.e., $\nu' \approx \nu_m$ in this limit.

As mentioned above, the coincidence of the wave spectrum with the peak position of the imaginary part of the Fourier transform of the Green function is observed when the mass operator depends weakly on the frequency. Indeed, Eq. (15) for the mass operator implies that at large k_c, the second term in the denominator on the right-hand side of this equation can appear much in excess of the first term; as a result, frequency dependence $\Sigma(k, \nu)$ becomes weaker. This situation can be implemented, first of all, at the values of the variables in Eq. (15) which correspond to the minimal value of the function g. Since $g = \bar{G}^{-1}(k, \nu)$, it follows that g is small at the values of k and ν corresponding to a high value of the Green function. In particular, this domain of the variables includes such important characteristics of the Green function as peak position ν_m of function $|\bar{G}''(k, \nu)|$ and the positions of the points which determine peak width $\Delta\nu$. This allows us, at large k_c, to disregard the first term in the denominator of Eq. (15) as compared to its second term. In this case, the mass operator is frequency-independent ($\Sigma(\nu, k) \approx \Sigma(k)$), and expression (15) yields the differential equation

$$\Sigma(k)\frac{d\Sigma(k)}{dk} + 2k\Sigma(k) + \frac{i\eta^2}{k_c} = 0, \quad (26)$$

which can be reduced to the special Riccati equation. The partial solution to this equation obtained under the condition $\Sigma(k) \longrightarrow 0$ for $k \longrightarrow \infty$ has the form

$$K = -i\sqrt{\xi}\frac{H_{-2/3}^{(1)}(s)}{H_{1/3}^{(1)}(s)}, \quad (27)$$

where $\xi = \tilde{\Sigma}(k) + K^2$, $s = 2K_c\xi^{3/2}/3$, and $H_\alpha^{(1)}(s)$ is the Hankel function. The numerical solution of Eq. (27) for $\tilde{\Sigma}(k)$ allows us to find the dependences of ν_m and

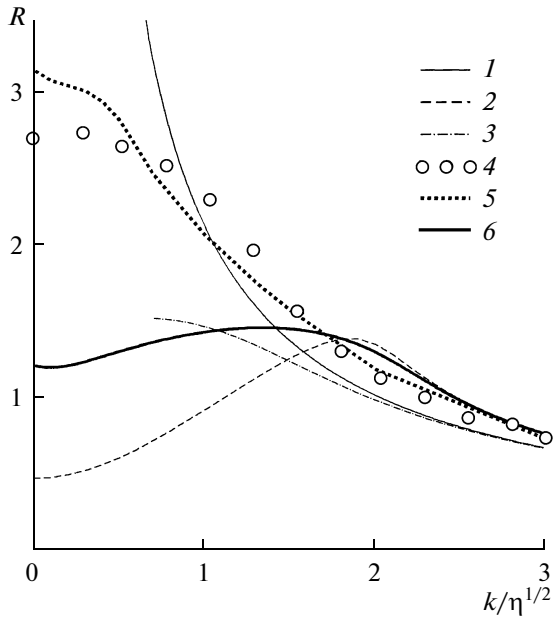

Fig. 8. Wave damping ν'' and width $\Delta\nu$ of the peak of function $|\bar{G}''(k, \nu)|$, $R = 2\nu''/\eta$ (curves *1–3*, *6*, *7*), $R = \Delta\nu/\eta$ (curves *4*, *5*); (*1–3*) ν' and ν'' are defined by formulas (8), (12), and (13); (*4*) ν_m and $\Delta\nu$ are obtained in [20]; (*5*) ν_m and $\Delta\nu$ are defined by formulas (9), (16), and (18); (*6*) ν' and ν'' are defined by formula (20); $k_c/\sqrt{\eta} = 0.5$.

$\Delta\nu$ on k (curves *6* in Figs. 2 and 3, respectively). Comparing curves *6* and the sequences of points *4* in these figures, we arrive at the conclusion that qualitative agreement exists in the behaviors of ν_m and $\Delta\nu$ as functions of k determined using expression (27) and in [20]. In this case, ν_m and $\Delta\nu$ can be directly expressed in terms of the mass operator: $(\nu_m - k^2)/\eta = \tilde{\Sigma}'(k)$, $\Delta\nu/\eta = -2\tilde{\Sigma}''(k)$. Expanding the right-hand side of Eq. (27) into a power series at low values of variable s and solving the resultant algebraic equation for $\tilde{\Sigma}(k)$ at $K \ll 1$, we obtain

$$\tilde{\Sigma}(k) \approx \frac{A(1+i\sqrt{3})}{K_c^{2/3}} + \frac{2\pi^2(\sqrt{3}+i)}{3^{1/6}\Gamma(2/3)bK_c^{1/3}}K. \qquad (28)$$

Here,

$$A = \frac{3^{5/3}\Gamma(2/3)\pi[b - 3\sqrt{3}\Gamma^3(2/3)]}{2(4\sqrt{3}\pi^3 - b^2)} \approx -0.5553,$$

where $b = [16\sqrt{3}\pi^3 - 81\Gamma^6(2/3)]^{1/2}$, $\Gamma(\tau)$ being the gamma function. The right-hand side of formula (28) coincides with the first two terms on the right-hand side of expression (23) to within a constant. This coincidence becomes complete if we apply to Eq. (26) the approximate method used for solving Eq. (15). Following this method, we express $\Sigma(k)$ from Eq. (26) and differentiate the result with respect to k. Assuming that $|d^2\Sigma(k)/dk^2|/2 \ll 1$, we eliminate the second derivative, which yields the following cubic equation for Y:

$$Y^3 - 2KY^2 - \frac{2i}{K_c} = 0. \qquad (29)$$

Only one solution of this equation is of physical interest,

$$Y = \frac{1}{3}\left[\left(\frac{D}{K_c}\right)^{1/3} + 4K^2\left(\frac{K_c}{D}\right)^{1/3} + 2K\right], \qquad (30)$$

where

$$D = 8K^3K_c + 27i + 3i\sqrt{3(27 - 16iK^3K_c)}.$$

Therefore, according to Eq. (26) subject to definition (17), we get

$$\tilde{\Sigma}(k) = -\frac{i}{K_cY}, \qquad (31)$$

where Y is described by formula (30). We find from expression (31) that $|d^2\Sigma(k)/dk^2|/2 < 0.2$ at $K_c \geq 0.5$. The $\nu_m(k)$ and $\Delta\nu(k)$ dependences, where $\tilde{\Sigma}(k)$ is defined by expression (31), are shown by curves *7* in Figs. 2 and 3, respectively. The behavior of these functions also qualitatively coincides with the results of [20] (sequence of points *4* in Figs. 2 and 3). At $K \ll 1$, we obtain from relations (30) and (31)

$$\tilde{\Sigma}(k) \approx -\frac{1+i\sqrt{3}}{(4K_c)^{2/3}} + \frac{\sqrt{3}+i}{3(4K_c)^{1/3}}K + O(K^3). \qquad (32)$$

Comparing formulas (23) and (32), we see that the first two terms on their right-hand sides are the same. In the case of uniform oscillations, the $\nu_m(k_c)$ dependence which follows from relations (30) and (31) is shown in Fig. 4, curve *4*. We note the closeness of curves *2–4* in this figure at $K_c \geq 1.5$, as well as their complete coincidence at $K_c \gg 1$. Thus, we can rightfully use Eq. (26) instead of Eq. (15) in the range of large K_c. Along with this, curves *2–4* in Fig. 4 at $K_c \geq 1$ demonstrate that the dependences they illustrate deviate from the numerical results of [20] (sequence of points *1* in this figure). Moreover, for the $\nu_m(k)$ dependences derived here, the inequality $\nu_m - k^2 < 0$ is valid at arbitrary k, while the numerical results of [20] give the sign reversal in this inequality upon an increase in k.

These discrepancies can be eliminated if we use three terms of expansion (14) in the denominator of the integrand in Eq. (10). Substituting them into Eq. (10), assuming that $|d^2\Sigma(k)/dk^2|/2 \ll 1$, and performing the integration, we obtain

$$\tilde{\Sigma}(k, \nu) = \frac{1}{\tilde{g} - iYK_c + K_c^2} - \frac{2iK_c}{(K_c^2 + \kappa_+^2)(\kappa_+ - \kappa_-)}, \qquad (33)$$

where

$$\kappa_\pm = -Y/2 \pm \sqrt{Y^2/4 + \tilde{g}}; \quad \mathrm{Im}(\tilde{g}/Y) > 0,$$
$$\mathrm{Im}(Y) > 0.$$

It is difficult to solve this equation; however, at $K_c \gg 1$, when the inequalities $4\tilde{g}/Y^2 \ll 1$ and $\tilde{g}/K_cY \ll 1$ are valid, relation (33) can be simplified like it was performed above for Eq. (15). Thus, in the range of large K_c, relation (33) can be reduced to the form

$$\tilde{\Sigma}(k) \approx -\frac{i}{K_cY} + \frac{1}{Y(Y + iK_c)}. \qquad (34)$$

This formula does not contain any dependence on frequency ν, as well as expressions (26) and (31) which follow from Eq. (15) if $K_c \gg 1$. The first term in relation (34) can be obtained taking into account only two terms of expansion (14) in Eq. (10) and coincides with the right-hand side of equality (31), while the second term appears when three terms of expansion (14) are taken into account in Eq. (10). If we consider the second term in relation (34) as a small addition to the first term and use formula (30) for Y, we obtain the $\nu_m(k)$ and $\Delta\nu(k)$ dependences presented, respectively, by curves *8* in Figs. 2 and 3. Therefore, if we take into account three terms of expansion (14) in Eq. (10), function $\nu_m - k^2$ appears to be alternating and agrees qualitatively with the results of numerical calculation (sequence of points *4* in Fig. 2) obtained in [20] throughout the domain of variable k. In the case of uniform oscillations, using the expression $Y = -(\sqrt{3} + i)/4AK_c^{1/3}$ for Y, which follows from formula (28) at $K = 0$, the $\nu_m(k_c)$ dependence which follows from relation (34) becomes

$$\frac{\nu_m}{\eta} = \frac{A(8A^2K_c^{8/3}+1)}{K_c^{2/3}(2AK_c^{4/3}+1)^2} \quad (35)$$

(see Fig. 4, curve *5*); $A \approx -0.5553$. It is seen that at $K_c \gg 1$, the results obtained in this paper coincide with the numerical data of [20] (cf. the sequence of points *1* and curve *5* in Fig. 4). Along with this, curve *5* successfully approximates the sequence of points *1* even at $K_c \geq 1$.

The Josephson plasma wave spectrum and damping at $K_c \gg 1$ can be obtained from relation (11), in which formula (34) is used for the mass operator. Since $\tilde{\Sigma}(k)$ is frequency-independent, we have $(\nu' - k^2)/\eta = \tilde{\Sigma}'(k)$ and $\nu''/\eta = -\tilde{\Sigma}''(k)$. At $K \gg 1$, relations (11) and (34) subject to definitions (17) for the wave spectrum and damping yield

$$\omega^2 \approx \omega_J^2\left[1 + \gamma^2\frac{1}{4(k\lambda_J)^2} - \gamma^2\frac{i}{2kk_c\lambda_J^2}\right] + (kc_0)^2, \quad (36)$$

which coincides with the asymptotic form of expression (8) at $k \gg k_c$.

CONCLUSIONS

In this work, we have used the simple one-dimensional model of a Josephson junction, which made it possible to develop a method for studying Josephson plasma waves and to trace the main regularities in the effect of the random inhomogeneities on their spectrum and damping. To analyze Eq. (3), which describes such waves in a randomly inhomogeneous junction, we used the self-consistent approximation, which takes into account multiple wave scattering on inhomogeneities, according to which Fourier transform (9) of the averaged Green function can be expressed in terms of the mass operator governed by integral equation (10). The solution to this equation describes the contribution made by the Josephson plasma waves and a stochastic spread of randomly inhomogeneous parameter $\lambda_J^{-2}(y)$ to the Green function. The latter mainly concerns the peak width $\Delta\nu$ of function $|\bar{G}''(k, \nu)|$ and is known as the nonuniform (fluctuation) broadening. Therefore, the $\nu_m(k)$ and $\Delta\nu(k)$ dependences, which follow from the numerical solution of Eq. (10), cannot be unconditionally used to determine the averaged wave spectrum ν' and damping ν''. To search for the dispersion relation for the averaged waves, we used the simplification of Eq. (10), which ensures only a slight violation of its self-consistency. A criterion of admissibility of this violation is the correspondence of ν_m and $\Delta\nu$ numerically obtained from relations (9) and (10) and those determined using the simplifying assumptions in Eq. (10). This criterion is not satisfied by the approximations taking into account the first orders of perturbation theory (cf. curves *1–3* and the sequence of points *4* in Figs. 2 and 3), which made us search for other approaches to simplification of Eq. (10). Analysis of this equation led to the conclusion that the major contribution to the integral on its right-hand side is made by the neighborhood of point $k_1 = k$. Therefore, the denominator in the integrand of Eq. (10) was expanded into a power series in the vicinity of this point. The use of the first two terms of expansion (14) made it possible to attain, at $k_c \leq \sqrt{\eta}/2$, the qualitative agreement between the $\nu_m(k)$ dependences determined in [20] and those obtained from relations (9), (16), and (18) (cf. the sequences of points *4* and curves *5* in Figs. 2 and 7), as well as the $\Delta\nu(k)$ dependences (cf. the sequences of points *4* and curves *5* in Figs. 3 and 8). The results obtained from expressions (9), (16), and (18) for the $\nu_m(k_c)$ dependence, which was studied for the uniform oscillations ($k = 0$), coincide at $k_c \leq 0.4\sqrt{\eta}$ with the data of [20] (the sequence of points *1* and curve *2* in Fig. 4). The above-mentioned correspondence allowed us, using relations (16) and (18), to find the averaged wave spectrum ν' and damping ν'' (relation (20)). We note the qualitative agreement of the $\nu'(k)$ and $\nu_m(k)$ dependences obtained, respectively, based on relation (20) and formulas (9), (16), and (18) (curves *5* and *6* in Figs. 5 and 7) and their coincidence at $k \gg \sqrt{\eta}$. For uniform oscillations ($k = 0$), the $\nu'(k_c)$ and $\nu_m(k_c)$ dependences obtained from the same set of formulas agree qualitatively and coincide at $k_c \gg \sqrt{\eta}$ (curves *2* and *3* in Fig. 4).Meanwhile, the laws of variation of ν'' and $\Delta\nu$ obtained, respectively, from relation (20) and formulas (9), (16), and (18) differ considerably from each other at $k < \eta/k_c$, $k_c < K_{c0}\sqrt{\eta}$, where $K_{c0} \approx 0.4387$. In this range of the k and k_c values, wave damping $\nu'' = 0$ at $k = 0$ and increases linearly with k, passes through the maximum at $k = \eta/k_c$ (curve *6* in Fig. 6), while $\Delta\nu$ decreases monotonically with increasing k (curve *5* in Fig. 6). At $k_c > K_{c0}\sqrt{\eta}$, the nonmonotonic dependence $\nu''(k)$ is retained, but in this case $\nu'' \neq 0$ at $k = 0$ (curve *5* in Fig. 8). Such a considerable change in the damping of uniform oscillations at slightly varying k_c in the vicinity of critical value $k_{c0} = K_{c0}\sqrt{\gamma}/\lambda_J$ is due to a change in the relation between correlation radius r_c and λ_J, which determines the effect of inhomogeneities on the wave propagation. As k_c increases in the range $k_c > K_{c0}\sqrt{\eta}$, the $\nu''(k)$ dependence becomes monotonic with a linear drop at $k \ll \sqrt{\eta}$ and $k_c \gg \sqrt{\eta}$ (see formulas (23) and (24)). In the limit $k \gg \sqrt{\eta}$, the averaged wave spectrum and damping are determined by relation (25). The coincidence of ν' and ν_m at $k_c \gg \sqrt{\eta}$ in the case of uniform oscillations (curves *2* and *3* in Fig. 4) suggested a weak frequency dependence of the mass operator. This fact

allowed us to neglect the first term in the denominator of Eq. (15), to obtain differential equation (26), and to find its solution (27) from which the mass operator $\tilde{\Sigma}(k)$ was obtained and the behavior of the $\nu_m(k)$ and $\Delta\nu(k)$ dependences was determined (see curves *6* in Figs. 2 and 3, respectively). The approximate solution to Eq. (26) yielded analytic relation (31) for $\tilde{\Sigma}(k)$, which was used to plot ν_m and $\Delta\nu$ (see curves *7* in Figs. 2 and 3, respectively). To eliminate the discrepancy between the analytical and numerical results at $k \gg \sqrt{\eta}$, $k_c \gg \sqrt{\eta}$ (cf. the sequence of points *4* with curves *5–7* in Fig. 2 and the sequence of points *1* with curves *2–4* in Fig. 4), we took into account three terms in expansion (14) in the integrand of Eq. (10). In this case, the integration in Eq. (10) yielded expression (33) for the mass operator, which can be reduced to formula (34) at $K_c \gg 1$. On its basis, the $\nu_m(k)$ and $\Delta\nu(k)$ dependences were obtained (see Figs. 2 and 3, curves *8*). For uniform oscillations, relations (34) and (28) give formula (35) used to obtain the $\nu_m(k_c)$ dependence (Fig. 4, curve *5*), which agrees with the numerical results of [20].

We note that the derivative $d\Sigma(k, \nu)/dk$ appearing in expression (15) can be determined by differentiating Eq. (10) with respect to k and using expansion (14) in taking the integral on the right-hand side of the resultant equation. However, the double application of this expansion gives a rougher approximation. In particular, in this approach, $\nu_m - k^2 = 0$ (the sequence of points *8* in Fig. 5), and this agrees with the numerical results only in the limit $k_c \ll \sqrt{\eta}$. Nonetheless, a good agreement of $\Delta\nu$ calculated using this approach (the sequence of points *8* in Fig. 6) with that calculated using formulas (9), (16), and (18) (curve *5* in Fig. 6) sets the basis for the determination dispersion relation for the averaged waves. Thus, at $k_c \ll \sqrt{\eta}$, using derivative $d\Sigma(k, \nu)/dk$ in relation (15) calculated by differentiating Eq. (10), we obtain

$$X = -i(KK_c - \sqrt{K^2K_c^2 - 1}). \quad (37)$$

The wave spectrum and damping which follow from this equality and formulas (11) and (17) are shown by curves *7* in Figs. 5 and 6, respectively. They are close to curves *6* in these figures, which illustrate the wave spectrum and damping determined based on relation (20). At $KK_c \ll 1$ ($k \ll \eta/k_c$), relation (37) yields the linear law with respect to γ for the gap in the wave spectrum, as well as the linear dependence on k and k_c for the wave damping, which agrees with formula (22). For $k \geq \eta/k_c$, the wave spectrum which follows from formula (37) is determined by relation (5), while the damping reaches its maximum at $k = \eta/k_c$, decreases with increasing k, and coincides with the imaginary part of relation (25) at $k \gg \sqrt{\eta}$.

The averaged wave damping which follows from relation (20) or (37) makes it possible to estimate the nonuniform broadening contribution to $\Delta\nu$. Comparison of $\Delta\nu$ (the sequence of points *4* in Figs. 6 and 8) and $2\nu''$ (curves *6* and *7* in Fig. 6 and curve *6* in Fig. 8) implies that, at small k_c, $k \ll \sqrt{\eta}$, $\Delta\nu$ is mainly determined by the nonuniform broadening, while at $k \gg \sqrt{\eta}$, the wave damping makes the main contribution to $\Delta\nu$. At $k_c \gg \sqrt{\eta}$, the effect of random inhomogeneities on the wave spectrum and damping manifests itself differently. In particular, the uniform oscillation damping ($k = 0$) and the peak width of function $|\overline{G''}(k, \nu)|$ exhibit analogous dependences on k_c described by the power law ν'', $\Delta\nu \propto 1/k_c^{2/3}$.

The modification of the Josephson plasma wave spectrum obtained in this work can appear useful for the investigation of random inhomogeneities of the Josephson junction. To this end, we can use the linear term in the long-wavelength spectral region which was obtained in the limit of "short-range" inhomogeneities ($r_c \leq \lambda_J/\sqrt{\gamma}$) and depends on the stochastic parameters γ and k_c (relation (24)). At the typical values of λ_J in the junctions for Josephson plasma waves, the inhomogeneities with the characteristic size $r_c < 10^{-4}$–10^{-5} cm are "short-range." Alternately, in the application of Josephson plasma waves, it might become interesting that (as follows from relation (24)), due to the linear dependence of the wave frequency on k, its group velocity appears much higher than that in the homogeneous junction, $c_0\gamma^{2/3}(\lambda_J k_c)^{-1/3} \gg c_0\lambda_J k$, where $k \ll \sqrt{\eta} = \sqrt{\gamma}/\lambda_J$, when the inhomogeneities are taken into account. However, we notice that the linear term in the wave spectrum appears also when the Josephson junction plane is at an angle to the sample surface [23].

ACKNOWLEDGMENTS

The author is grateful to V.V. Val'kov, A.V. Vedyaev, A.G. Granovskii, and S.G. Ovchinnikov for useful discussions and valuable comments.

REFERENCES

1. Yu. Ya. Divin, U. Poppe, I. M. Kotelyanskii, V. N. Gubankov, and K. Urban, Radiotekh. Elektron. (Moscow) **53**, 1205 (2008).
2. S. Savel'ev, V. A. Yampol'skii, A. L. Rakhmanov, and F. Nori, Rep. Prog. Phys. **73**, 026501 (2010).
3. A. Barone and G. Paterno, *Physics and Applications of the Josephson Effect* (Wiley, New York, 1982; Mir, Moscow, 1984).
4. K. K. Likharev, *Introduction to Dynamics of Josephson Junctions* (Nauka, Moscow, 1985) [in Russian].

5. Yu. S. Kivshar', B. A. Malomed, and A. A. Nepomnyashchii, Zh. Eksp. Teor. Fiz. **94**, 356 (1988) [Sov. Phys. JETP **67**, 850 (1988)].
6. Yu. S. Kivshar and O. A. Chubykalo, Phys. Rev. B **43**, 5419 (1991).
7. F. Kh. Abdulov and E. N. Tsoi, Zh. Tekh. Fiz. **67** (8), 57 (1997) [Tech. Phys. **42**, 905 (1997)].
8. O. Yu. Andreeva, T. L. Boyadjiev, and Yu. M. Shukrinov, Physica C **460–462**, 1315 (2007).
9. L. Morales-Molina, F. G. Mertens, and A. Sanchez, Phys. Rev. E **72**, 016612 (2005).
10. A. A. Golubov and A. V. Ustinov, Pis'ma Zh. Tekh. Fiz. **12**, 435 (1986) [Sov. Tech. Phys. Lett. **12**, 178 (1986)].
11. B. A. Malomed, I. L. Serpuchenko, M. I. Tribel'skii, and A. V. Ustinov, Pis'ma Zh. Eksp. Teor. Fiz. **47**, 505 (1988) [JETP Lett. **47**, 591 (1988)].
12. B. A. Malomed, Phys. Rev. B **38**, 9242 (1988); **41**, 2616 (1990).
13. B. A. Malomed, V. A. Oboznov, and A. V. Ustinov, Zh. Eksp. Teor. Fiz. **97**, 924 (1990) [Sov. Phys. JETP **70**, 518 (1990)].
14. M. V. Fistul, P. Caputo, and A. V. Ustinov, Phys. Rev. B **60**, 13152 (1999).
15. E. G. Semerdzhieva, T. L. Boyadzhiev, and Yu. M. Shukrinov, Fiz. Nizk. Temp. **31**, 1110 (2005) [Low Phys. Temp. **31**, 847 (2005)].
16. M. B. Mineev, M. F. Feigel'man, and V. V. Shmidt, Zh. Eksp. Teor. Fiz. **81**, 290 (1981) [Sov. Phys. JETP **54**, 155 (1981)].
17. V. A. Ignatchenko and R. S. Iskhakov, Zh. Eksp. Teor. Fiz. **72**, 1005 (1977) [Sov. Phys. JETP **45**, 526 (1977)].
18. R. H. Kraichnan, J. Math. Phys. **2**, 124 (1961).
19. G. Brown, V. Celli, M. Haller, A. A. Maradudin, and A. Marvin Phys. Rev. B **31**, 4993 (1985).
20. V. A. Ignatchenko and V. A. Felk, Phys. Rev. B **71**, 094417 (2005).
21. R. C. Bourret, Nuovo Cimento **26**, 1 (1962); Can. J. Phys. **40**, 782 (1962).
22. S. M. Rytov, Yu. A. Kravtsov, and V. I. Tatarskii, *Introduction to Statistical Radio Physics* (Nauka, Moscow, 1978), Chap. 2.
23. A. I. Lomtev, Zh. Eksp. Teor. Fiz. **113**, 2256 (1998) [JETP **86**, 1234 (1998)].

Translated by E. Perova